[Frontiers in Bioscience 9, 2860-2872, September 1, 2004]

ACTIVATING THE RYANODINE RECEPTOR WITH DIHYDROPYRIDINE RECEPTOR II-III LOOP SEGMENTS: SIZE AND CHARGE DO MATTER

Marco G. Casarotto [1, 2], Daniel Green[1], Suzy Pace[1], Jaqui Young[1] and Angela F. Dulhunty [1]

[1] Division of Molecular Bioscience, John Curtin School of Medical Research, [2] Research School of Chemistry, Australian National University

TABLE OF CONTENTS

1. ABSTRACT

Excitation-contraction coupling in skeletal muscle is thought to depend on a physical interaction between II-III loop of the α_1 subunit of the skeletal dihydropyridine receptor (DHPR) and ryanodine receptor (RyR). A peptide corresponding to II-III loop residues 671-690 of the skeletal DHPR (peptide *A*) is a high affinity activator of the RyR when it adopts an α-helical structure with critical basic residues aligned along one helical surface (1). Neither the structure of the full length II-III loop, or of sequences longer than 671-690 residues have been determined. Here we describe the structure and function of a 40 amino acid peptide corresponding to residues 671-710 (peptide *AB*) of the skeletal DHPR α_1 subunit. This peptide contains the *A* region with a further 20 residues towards the C-terminus of the II-III loop. We predicted that peptide *AB* would strongly activate the RyR, because (a) it contains the active *A* sequence of basic residues and (b) it contains a greater proportion of the II-III loop. The structure of the *AB* peptide was determined and it was found to consist of two helical regions joined by an unstructured linker region. Surprisingly, although the structure of the *A* region was maintained, the 40 residue peptide was unable to release Ca^{2+} from skeletal SR. Strong activity was restored when four negatively charged residues in the C-terminal part of the peptide were replaced by neutral residues. The charge substitution caused minimal changes in the overall structural profile of the peptide and virtually no changes in the *A* portion of the peptide. The results suggest that the ability of the *A* region of the skeletal II-III loop to interact with the RyR could depend on the tertiary conformation of the II-III loop, which is thought to change during EC coupling.

2. INTRODUCTION

Protein-protein interactions between two Ca^{2+} channels, the dihydropyridine receptor (DHPR) and ryanodine receptor (RyR) are central to excitation-contraction (EC) coupling in skeletal muscle. The DHPR L-type Ca^{2+} channel in the transverse tubule membrane detects surface depolarisation and transmits a signal to the RyR channel in the sarcoplasmic reticulum (SR) via the cytoplasmic domains of the two proteins. This interaction initiates the release of Ca^{2+} from the SR, and this Ca^{2+} in turn acts on a series of proteins to result in contraction. Skeletal EC coupling is independent of an influx of Ca^{2+} ions through the DHPR, i.e. it is independent of extracellular Ca^{2+} concentration and of DHPR Ca^{2+} channel function. In contrast, cardiac EC coupling depends of Ca^{2+} entering the fiber through the DHPR and activating the RyR. One of the regions of the DHPR that is thought to interact with the RyR in skeletal muscle EC coupling is located in the II-III loop between the 2nd and 3rd transmembrane repeats in the α_1 subunit (2). A skeletal sequence in the loop is required for skeletal type EC coupling in myocytes (2). In addition, the recombinant II-III DHPR loop, as well as two small fragments of the loop, can activate RyR channels in lipid bilayers and SR vesicles (3-10). These fragments correspond to residues Thr^{671}-Leu^{690} (*A* region) and Glu^{724}-Pro^{760} (*C* region) (as

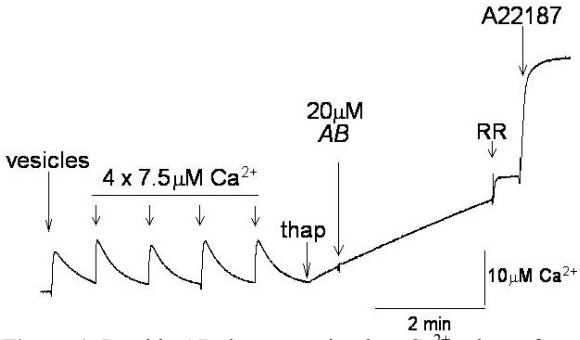

Figure 1. Peptide AB does not stimulate Ca^{2+} release from skeletal SR vesicles. The record shows absorbance as a function of time in an experiment assessing the ability of peptide AB to release Ca^{2+} from skeletal SR vesicles. The trace also illustrates the protocol followed in these experiments (see methods for additional details). SR vesicles were added to the cuvette at the start of the experiment. The vesicles were then partially loaded with Ca^{2+} by adding 4 aliquots of $CaCl_2$, each increasing the extravesicular Ca^{2+} concentration by 7.5 μM. Time was allowed between each addition for the added Ca^{2+} to be accumulated by the vesicles. Thapsigargin (200 nM) was then added to suppress Ca^{2+}, Mg^{2+}-ATPase activity, followed by peptide. The addition of peptide AB did not cause any significant increase in Ca^{2+} released from SR vesicles indicating that it did not activate the RyR1. Ruthenium red (RR) (5 μM) showed that Ca^{2+} release was through the RyR. The Ca^{2+} ionophore, A23187 (3 μg/ml) released Ca^{2+} remaining in the SR vesicles.

defined in (6)). We have previously identified key sequence and structural elements of the DHPR II-III loop *A* region that underpin the molecular recognition of the RyR and its ability to either activate the RyR with high affinity or to induce a low affinity voltage-dependent inhibition (1, 11, 12). The pre-requisite for activation, is that a series of lysine and arginine (RKRRK) residues are aligned and form a positively charged surface. The positively charged surface in the *A* peptides requires a helical structure. In contrast, two RyR-activating toxins (imperatoxin A and maurocalcine), that are thought to bind to the same site as peptide *A* (5, 7) , present a spatially similar positively charged surface on a β-sheet template. Inhibition by the *A* peptides requires the same set of positive charges but with a random coil structure.

The 20 amino acid peptide *A* is the largest fragment of the II-III loop whose structure has been solved experimentally. Here we describe the solution structure of a 40 residue peptide (*AB*) which corresponds to residues 671-710 of the skeletal DHPR α1 subunit. This larger peptide, including the *A* region plus a further 20 amino acids towards the C-terminus of the II-III loop, was examined (a) to extend the structural study of the II-III loop and (b) to determine whether the additional residues may further stabilize the structure and activity of the *A* region. The 40 amino acid peptide in fact lost the ability to activate the RyR even though the fragment remained highly helical, particularly in the *A* region. Replacement of four acidic residues in C terminal half of the *AB* peptide with uncharged moieties rendered the peptide capable of activating the RyR. These functional changes depended solely on the charge of the residues and were not associated with any gross structural change.

3. METHODS

Peptides were synthesised and purified as described in (4). Peptides used were:

AB – ^{671}TSAQKAKAEE RKRRKMSRGL PDKTEEEKSV MAKKLSQKPK^{710}

AB_{CH} – ^{671}TSAQKAKAEE RKRRKMSRGL P**A**KT**AVA**KSV MAKKLSQKPK^{710}

AB_{LK} - ^{671}TSAQKAKAEE RKRRKMSRGL **A**D**A**TEEEKSV MAKKLSQKPK^{710}

3.1. NMR

Peptides were dissolved at ~2-3 mM in 10% D_2O/90% H_2O and pH adjusted to a value of 5. ^{1}H chemical shift values are relative to 2, 2-dimethyl-2-silapentane-5-sulfonate. In order to enhance the spectral resolution, all further samples, including the peptide AB and AB mutants were dissolved in d_{18}-trifluroethanol 18% /82% H_2O. Spectra were acquired on a Varian-Inova 600 spectrometer using a spectral width of 6000 Hz, a pulse width of 7 μs (90°), and acquisition time of 0.130 s, collecting 4096 data points and 512 increments of 32 transients. NOESY (13) spectra (mixing time of 200-500 ms), TOCSY (14) spectra (mixing time of 70 ms) and DQF-COSY (15) spectra were acquired at 298 K and used for the assignment of the 1H-NMR resonances. Suppression of the H2O resonance for the NOESY, TOCSY and DQF-COSY spectra was achieved using pulse field gradients (16, 17). Temperature coefficients (16) and hence the patterns of backbone hydrogen bonding were assessed by monitoring the chemical shift values of the amide backbone protons with changes in temperature (277, 285, 298 K) in the DQF-COSY and TOCSY experiments. 2D data were processed on an O2 Silicon graphics work station using Felix 98 software. Data sets were zero-filled to 4096 by 2048K and multiplied by a phase-shifted sine-bell-squared function in both dimensions prior to transformation. $^3J_{NH-\alpha H}$ coupling constants were derived from 1D and 2D DQF-COSY ^{1}H spectra.

3.1.1. Structure Calculations

Distance constraints were derived manually from a 2D NOESY spectrum acquired with a mixing time of 200 ms. Upper bounds were derived from NOE crosspeak intensities by counting the number of contour levels of non-overlapped crosspeaks and using distances calibrated from Gln γ-methylene protons. NOE signals were classified into four categories of upper distance limits of 2.7, 3.5, 4.5 and 5.8 Å, each with a 1.9 Å lower distance limit. Dihedral angle restraints based on the $^3J_{NH-H\alpha}$ measurements were included in the final calculations with a tolerance of 20°.

Structure calculations were performed with the X-PLOR program (17, 18), using the *topallhdg.pro* topology file and *parallhdg.pro* parameter file, with the simulated annealing protocol on a Silicon Graphics O2

workstation. The sum averaging option was used to treat equivalent and non-stereospecifically assigned protons. Calculations were iterative, checking violations after each round and adding or refining constraints. Hydrogen bonds were identified and introduced after initial calculations. These were simulated by a 3.3 Å restraint between the amide nitrogen and carbonyl oxygen and a 2.3 Å restraint between the amide hydrogen and the carbonyl oxygen. Initially, 100 fully extended structures with random coordinates were generated. Structures were analysed and 17 selected for distance and dihedral constraint violations and low energies. No structures had NOE violations >0.5 Å or dihedral violations >5°. For structural comparisons, individual structures were superimposed onto the average structure.

3.2. Circular Dichroism

Peptide samples were diluted to 25 μM for CD measurements in 100% H_2O or 82% H_2O/18 % TFE and the pH values adjusted to 5. CD spectra were collected at 5° C on a Jobin Yvon CD6 Dichrograph using a cell path length of 1 mm. Ten spectra were collected per sample, averaged and then subjected to a smoothing function.

3.3. Ca^{2+} release

Preparation of SR vesicles and measurements of Ca^{2+} release from SR and have been described (4). Rabbit skeletal SR vesicles (100 μg of protein) were added to a cuvette, to a final volume of 2 ml of a solution containing (in mM): 100, KH_2PO_4 (pH = 7); 4, $MgCl_2$; 1, Na_2ATP; 0.5, antipyrylazo III. Extravesicular (Ca^{2+}) was monitored at 710 nm. Identical experiments at 790 nm (to test for non-Ca^{2+}-dependent changes in absorbance that may be induced by peptide) showed no changes in OD which would alter the rate of Ca^{2+} release measured at 710 nm.

4. RESULTS

The ability of peptide AB to release Ca^{2+} from skeletal SR The 40 amino acid '*AB*' peptide, contains the 20 amino acid *A* region (residues 671-690) of the skeletal DHPR α_1 subunit, plus the adjoining 20 amino acids from the *B* region (residues 691-710). Although it was anticipated that peptide *AB* would release Ca^{2+} with an efficacy equivalent to or greater than that of peptide *A*, the 40 residues peptide was inactive.

4.1. The structure of peptide AB

The following structural analysis showed that peptide *AB* has two distinct helical components joined by an unstructured linker region. When the vehicle for the peptide was H_2O, both NMR and CD analysis suggested that the peptide had a significant proportion of α-helical structure. The crosspeaks between adjacent amide backbone protons in the NOESY spectra strongly suggest helical structure (Figure 2A). The CD spectra of α-helical proteins would generally display a maximum at 196 nm, and minima at 208 nm and 222 nm. A minimum for peptide AB at ~198 nm and a slight dip at 219 nm (Figure 2C) indicates a mixture of α-helix and random coil. Addition of TFE (18%), to stabilise the secondary structure and allow structure determination (19, 20), increased NMR spectral resolution, decreased the peak linewidth in the NOESY spectrum (Figure 2B), and shifted one CD minimum from 198 to 204 nm and enhanced the minimum at 222 nm (Figure 2C).

A full NMR ^1H assignment was performed in an 18% TFE/82% H_2O mixture. Cross peaks between the amide ^1H atoms of adjoining residues (*i - i+1*) and/or for (*i – i+2*), indicated two distinct regions of α-helical structure between residues 1-14 and 23-36 (Figure 2B). The helical content was also assessed from: (i) coupling constants, (ii) α-^1H chemical shifts, and (iii) temperature coefficients (Table 1). Coupling constants from one-dimensional ^1H spectra and/or one-dimensional slices from DQF-COSY spectra of ≤ 6.1 Hz between the first 12 residues and between 23-33 were indicative of α-helices. α-^1H chemical shifts for residues 1–14 and 23–33 were upfield from those observed for random coil structure (Table 1) (21). Temperature co-efficients of amide ^1H chemical shifts were measured over a temperature range of 21° K. Values of >–5 ppb/K indicated hydrogen bonding between the backbone carbonyl oxygen and amide protons in an α-helix.

The NOESY spectrum yielded 414 distance constraints (Table 2) from which 100 possible structures were calculated in conjuction with the coupling constants (8) and hydrogen bonds (10). The backbone heavy atoms of the17 lowest energy structures were overlaid and an average structure calculated (Figure 3). The structures show two regions of α-helix, connected through an unstructured linker between residues 17-22. The lack of medium or long range NOE connectivities in the linker region suggested that this region was structurally disordered.

To summarise, peptide AB was functionally inactive even though the α-helical structure of the activating A region was retained. This could have been due to acidic residues in the B region preventing the basic *A* residues from interacting with their activating site on the RyR, either because (a) the flexible linker allowed the two helices to interact and shield the active A residues or (b) the negative charge in the B region prevented the A region from interacting appropriately with its binding site. To test these possibilities, two mutant peptides were designed. In the first peptide, AB_{LK}, the proline and lysine residues in the linker sequence L**P**D**K**T (residues 20-23) were substituted to give the mutant sequence L**A**DA**A**T. In the second peptide, AB_{CH}, negatively charged residues in the **D**KT**EEE**K sequence (residues 22-28) in the *B* region were altered to give a mutant sequence **A**KT**AVA**K.

4.1.1. Ca^{2+} release by mutant peptides

AB_{LK} like peptide AB, did not cause any substantial increase in Ca^{2+} release from SR vesicles (Figure 4A). There was however a small increase in release rates with $\boldsymbol{AB_{LK}}$, with slopes of ~7 nmoles/mg/min which were significantly greater that the negative slopes of ~-5 nmoles/mg/min with the native *AB* (since the slope in thapsigargin was subtracted from the slope after peptide addition, a small negative value was obtained if vehicle was added alone or if the peptide had no effect). In contrast to

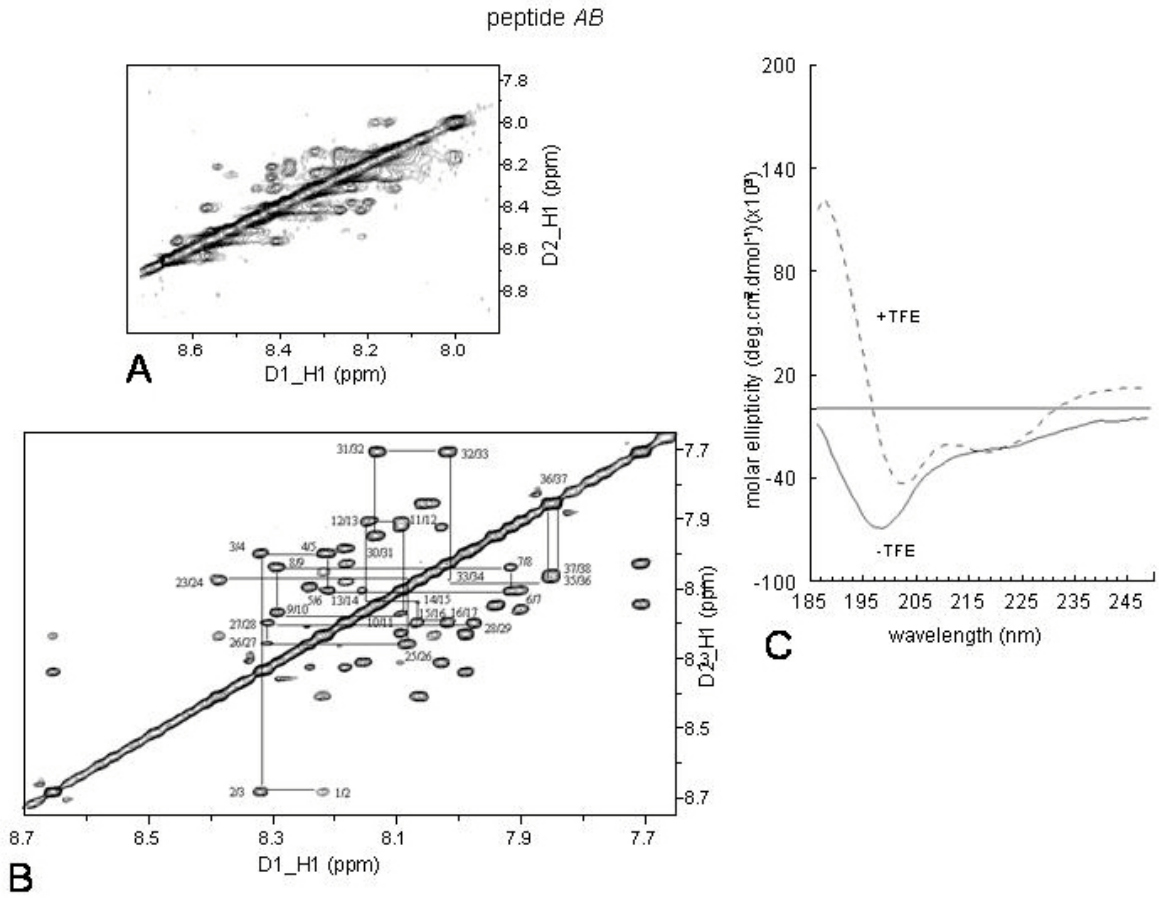

Figure 2. NMR and CD analysis of the AB peptide indicate a strong helical structure. The amide-amide region of the AB peptide NOESY spectrum in 90%D_2O/10%H_2O is shown in (**A**). A similar region of the spectrum is shown for the AB peptide in 82% H_2O/18 % d_{18} TFE mixture in (**B**), where strong and continuous i-i+1 NOEs are shown and correspondingly labeled (1-17 and 23-38). (**C**) CD spectra at 5°C for the AB peptide in 100% H_2O (solid line) and 82% H_2O/18 % TFE (dashed line).

AB and AB_{LK}, AB_{CH} activated a strong Ca^{2+} release from the SR, at concentrations as low as 0.5 μM (Figure 4B&C). The rate of release of Ca^{2+} increase with increasing AB_{CH} peptide concentration, approaching a maximum with 60 `M peptide. Thus, altering the amino acid composition of the linker region allowed a very small recovery of activity, while removing negative charges from the ***B*** region allowed recovery of activity that was substantially greater than that of the native A1 peptide (Figure 4C).

4.2. The structure of peptides

4.2.1. AB_{CH} and AB_{LK}

The functionally inactive AB_{LK} contained more secondary structure than the wild type *AB*. There were 36 $NH_i - NH_{i+1}$ NOE cross peaks in the amide-amide region of the NOESY spectrum, compared with 24 for the wild type peptide (Figure 5A). $NH_i - NH_{i+1}$ cross peaks were continuous from residue 1-23 and from 24-36. The α-helical content was also indicated by chemical shift and α-^{1}H CSI values (Table 3). Indeed the α-^{1}H values were consistent with α-helical structure from residues 1 to 35. Thus the linker region (residues (17-21) which was previously disordered has been incorporated into the α-helix. CD analysis also showed that AB_{LK} contained alpha helical secondary structure. In the absence of TFE, the CD spectrum had a minimum at 200 nm and an inflexion at 218 nm, suggesting a mixture of random coil and α-helix (Figure 5B). In the presence of 18% TFE, the maximum shifted to 188 nm and there were minima at 205 and 220 nm (Figure 5B). The positions of the maximum and minima, and the depth of the minimum at 219 nm, suggest AB_{LK} contained the greatest α- helical secondary structure of the three *AB* peptides.

The structural profile of the functionally active AB_{CH} was similar to that of the wild type *AB* peptide. There were amide ^{1}H backbone NOE connectivity's between adjoining residues from 1-14 and from residues 22-36 (Figure 6A). NOEs were absent between residues 17-22 indicating that the mutant peptide retained the unstructured linker region of peptide *AB*. The NH chemical shifts and α-^{1}H deviations for the majority of residues in the AB_{CH} (Table 4) were similar to those in *AB*, implying that the secondary structure was conserved in the two peptides. The CD spectra indicated the usual increase in structure after TFE addition, with the appearance of a maximum at 188 nm and a shift in the minima to 204 and a more pronounced minima at 220 nm (Figure 6B).

Table 1. Proton NMR assignment (p.p.m.), coupling constants (Hz) and Temperature coefficients (p.p.b./K) for the AB peptide in 18 % TFE, pH 5.0 at 25°C

Residue	NH	Hα	Hβ	Other	$^3J_{(NH-\alpha H)}$ (Hz)	Temp Co. (ppb.K^{-1})
Thr^{671}	8.22	4.47	4.39	Hγ 1.32		-12.8
Ser^{672}	8.66	4.33	3.98/4.04		4.5	-4.1
Ala^{673}	8.32	4.24	1.46			-8.0
Gln^{674}	7.99	4.07	2.45/2.48	Hγ 2.48/2.45, δNH$_2$ 7.44/6.80		-2.5
Lys^{675}	8.22	4.07	1.90	Hγ 1.56, Hδ 1.71, Hε 2.96, eNH$_2$ 7.60		-2.8
Ala^{676}	8.10	4.16	1.51			-1.8
Lys^{677}	7.92	4.08	1.92	Hγ 1.47,Hδ 1.63/1.73,Hε 2.98,eNH$_2$ 7.61	4.9	-4.5
Ala^{678}	8.03	4.23	1.54			-3.2
Glu^{679}	8.30	4.11	2.18/2.25	Hγ 2.61/2.53	6.1	-1.2
Glu^{680}	8.16	4.11	2.21/2.23	Hγ 2.51/2.59	4.7	0.0
Arg^{681}	8.10	4.04	1.86/1.96	Hγ 1.65/1.78, Hδ 3.23, NH 7.30		-3.2
Lys^{682}	7.90	4.07	1.96	Hγ 1.44,Hδ 1.58/1.73,Hε 3.00,eNH$_2$ 7.60	5.3	-3.0
Arg^{683}	8.14	4.12	1.84/1.94	Hγ 1.66/1.78, Hδ 3.22, NH 7.26		-3.3
Arg^{684}	8.13	4.17	1.81/1.93	Hγ 1.69, Hδ 3.21, NH 7.28		-1.5
Lys^{685}	8.07	4.20	1.83/1.94	Hγ 1.58, Hδ 1.63, Hε 3.01, eNH$_2$ 7.62		-0.5
Met^{686}	8.18	4.44	2.12/2.20	Hγ 2.62/2.72, εCH$_3$ 2.20		-1.4
Ser^{687}	8.02	4.45	3.96/4.00			-3.4
Arg^{688}	8.05	4.38	1.86/1.98	Hγ 1.70/1.77, Hδ 3.24, NH 7.24		-8.2
Gly^{689}	8.22	4.00				-6.0
Leu^{690}	7.99	4.66	1.69/1.71	Hγ 1.60, Hδ 0.98/0.96		-16.9
Pro^{691}		4.67	2.35	Hγ 2.06, Hδ 3.67/3.85		
Asp^{692}	8.05	4.24	1.88			-13.2
Lys^{693}	8.39	4.24	1.91	Hγ 1.48/1.53, Hδ 1.74, Hε 2.99	5.7	-7.6
Thr^{694}	8.07	4.28	4.12	Hγ 1.29		-15.7
Glu^{695}	8.09	4.14	2.13/2.17	Hγ 2.53/2.54		-0.2
Glu^{696}	8.25	4.16	2.01/2.19	Hγ 2.55/2.47	5.3	-1.6
Glu^{697}	8.31	4.07	2.17/2.26	Hγ 2.62/2.50		-0.5
Lys^{698}	8.19	4.07	1.92	Hγ 1.46, Hδ 1.67, Hε 2.95, eNH$_2$ 7.60		-2.6
Ser^{699}	7.98	4.30	4.01/4.06			-5.0
Val^{700}	7.95	3.79	2.22	Hγ 0.99/1.09		-3.3
Met^{701}	8.14	4.24	2.16	Hγ 2.62/2.70		0.0
Ala^{702}	8.13	4.30	1.51			-2.0
Lys^{703}	7.71	4.11	1.72/1.95	Hγ 1.49, Hδ 1.62, Hε 3.01, eNH$_2$ 7.58	5.5	-7.1
Lys^{704}	8.02	4.15	1.95/1.98	Hγ 1.47/1.50,Hδ 1.71,Hε 2.98,eNH$_2$ 7.61		-3.2
Leu^{705}	8.06	4.26	1.62	Hγ 1.57, Hδ 0.90/0.93		0.0
Glu^{706}	7.86	4.35	2.06/2.19	Hγ 2.54/2.63		-9.2
Gln^{707}	7.85	4.29	2.06/2.17	Hγ 2.42/2.54, Hδ 6.80/7.50		-8.9
Lys^{708}	8.05	4.62	1.81/1.87	Hγ 1.53,Hδ 1.72/1.74,Hε 3.05,eNH$_2$ 7.58		-8.2
Pro^{709}		4.47	2.06/2.35	Hγ 1.94, Hδ 3.67/3.87		
Lys^{710}	8.32	4.29	1.88	Hγ 1.51, Hδ 1.76, Hε 3.05, eNH$_2$ 7.61		-4.5

It is clear that, apart from the extra helical content in the centre of the AB_{LK} peptide, there is very little difference in the secondary structures of the mutant and wild type peptides. It is significant that the *A* region, containing the critical positively charged residues (11-15), is structurally similar in all 3 peptides.

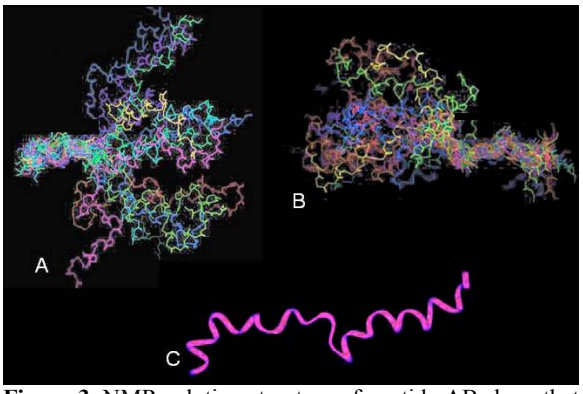

Figure 3. NMR solution structure of peptide AB show that it contains two helical tails connected by a linker region. Since it was not possible to overlay all backbone residues for the 17 structures, a best fit superposition of backbone heavy atoms of either residues Gln^{671}-Arg^{684} (**A**) or (and Lys^{693}-Gln^{707} (**B**) was performed. The average structure was calculated and is shown in (**C**).

Table 2. Summary of NOE, coupling constants and hydrogen bond restraints for the AB peptide

Restraints	**Peptide A1-D18**
Total NOEs	414
Intra	238
$i-(i+1)$	106
$i-(i<1)$	70
$^3J_{NH-H\alpha}$	8
Hydrogen Bonds	10

5. DISCUSSION

We show here that the 40 residue *AB* peptide, corresponding to the N-terminal part of the II-III loop in the α_1 subunit of the skeletal muscle dihydropyridine receptor, is incapable of activating the skeletal RyR1. This result was surprising because (a) the first 20 residues of the peptide were identical to those comprising the smaller *A* peptide which is a high affinity activator of the Ca^{2+} release channel and (b) the structure of the *A* region in the 40 residue peptide was very similar to the structure of the *A* peptide. The results of mutation analysis indicate that the loss of function is primarily due a group of negatively charged residues in the C-terminal half of the 40 residue peptide. Replacement of these residues with uncharged amino acids resulted in the full recovery of activity. These unexpected findings emphasize that changes in peptide length can cause functional changes when small protein fragments are examined.

5.1. Structural requirements for RyR activation by the A region of the II-III loop

The conformation of the *A* peptide is a critical determinant for its molecular recognition of the RyR and its ability to initiate Ca^{2+} release. The structural requirement is for alignment of key positively charged residues along one surface of the α-helix of the peptide (1, 11, 12). This alignment is similar to that of positively charged residues on the surface of the β-sheet scorpion toxins, imperatoxin A and maurocalcine (1, 22), which are thought to activate the RyR by binding to the same site as the *A* peptide (5, 7). The key residues in the *A* peptide are a part of the RKRRK cluster (residues 11-15). Only 4 of these 5 residues are required for RyR activation, since the cardiac *A* peptide with an equivalent sequence, KERKK, activates the RyR in the same way as skeletal peptide (23, 24). The cardiac and skeletal *A* sequences share a similar α-helical structure (23), that allows the alignment of at least 3 of the basic residues along the surface of the peptide's α-helix (1).

5.2. Structure and function of the AB peptide

The inactive *AB* peptide has two distinct helical components joined by an unstructured linker region. Since the important α-helical structure including the RKRRK sequence (residues 11-15), and the global orientation of the positively charged residues, is retained in the 40 residue peptide, structural disruption of the *A* region cannot explain the *AB* peptide's loss of activity. An alternative hypothesis is that the tertiary structure of the peptide allows an interaction between the two oppositely charged helices in the *AB* peptide preventing the positively charged *A* region from interacting with the RyR. The linker region including residues 18-22 would have to adopt a hairpin turn for the two helices to physically interact. Although no NOE evidence was found to support this hypothesis, the structural nature of the linker region, containing a glycine and proline residue could be such that the two helices could potentially interact.

We tested the hypotheses that (a) the negative charge density in the C-terminal half of the AB peptide was important in abolishing the activity of the A region and (b) that the flexibility of the linker region allowed a direct interaction between the oppositely charged helices. In the first case the charge distribution of the second (*B*) helix was altered in the AB_{CH} peptide by substituting neutral for negatively charged residues. In the second case, the sequence of the linker region was altered in the AB_{LK} peptide to affect the structural profile and influence the potential interactions between the two helices. The α-helix was extended into the linker region in AB_{LK}. Although the mutations did not cause any major change in the structure of the two α-helical regions, AB_{CH} induced significant calcium release which was in fact greater than that induced by peptide *A*, and equivalent to release by the most active of the A peptides - A1(D-R18) (1). On the other hand AB_{LK} remained inactive, even though its α-helical structure was if anything stronger than that in AB_{CH}.

These results indicated that a cluster of negatively charged *B* residues prevented the basic *A* residues from activating with the RyR, but that this interaction did not depend on the structural and dynamic characteristics of the linker. Thus the overall charge of the wild type *AB* peptide was such that the *A* region could no longer bind to its activation site. If the *A* region of the full 2-3 loop binds to the same site on the RyR as peptide *A*, then the tertiary structure of the full loop must be such that the effect of the negatively charged residues in the *B* helix on the *A* region is diffused.

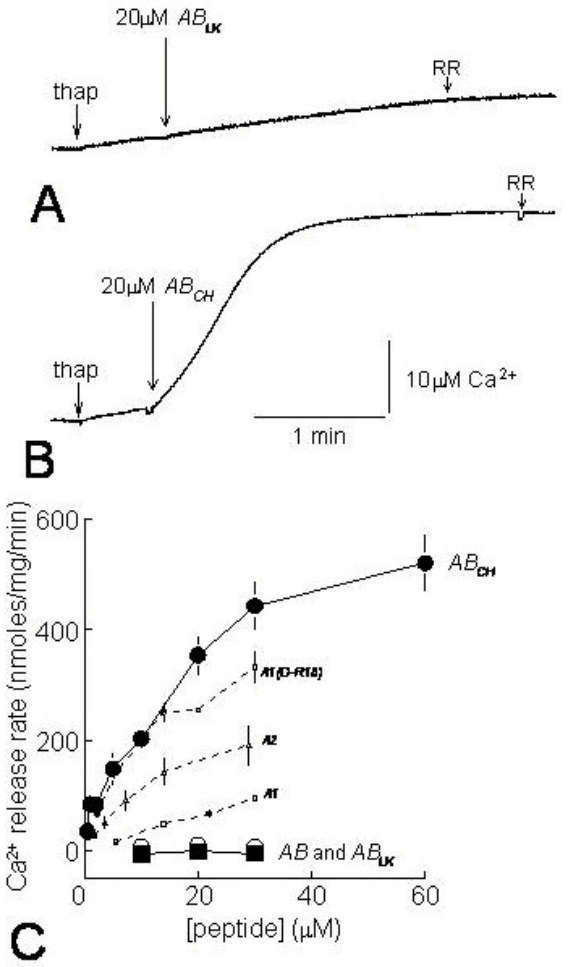

Figure 4. Mutations in the linker region of peptide AB do not restore the activity of the A region, but removal of negatively charged residues in the C terminal half of the peptide result in recovery of a strong activity. (**A**) is a record of absorbance as a function of time showing that peptide AB_{LK} (20 μM), added ~1 min after thapsigargin, fails to induce substantial Ca^{2+} release from skeletal SR vesicles. (**B**) shows that peptide AB_{CH} at 20 μM induces strong Ca^{2+} release. (**C**) – rates of Ca^{2+} release in nmoles/mg/min as a function of peptide concentration. Average data is given for peptide AB (large filled squares), AB_{LK}, (large open circles) and AB_{CH} (large filled circles). Also included for comparison are average rates of Ca^{2+} release with the native A peptide A1 (small open squares, (4)), mutant peptide A2 (small open triangles (4), and mutant peptide A1(D-R18) (small open circles (1)).

5.3. The structure of the AB region in the full II-III loop

An important finding in this study was that addition of 20 C-terminal residues to the *A* peptide did not alter the helical structure of the *A* region. Furthermore, our preliminary analysis of the recombinant 126 residue II-III loop shows two helices in the *AB* region (Dulhunty and Casarotto, unpublished data), equivalent to those seen in the *AB* peptide. The predicted structure of the full II-III loop also indicates that there two helices in the same position (24). Other regions of the II-III loop also retain their structural integrity when isolated from the larger protein. A peptide corresponding to residues 725-760 (i.e. the *C* region of the II-III loop as defined by El-Hayek *et al*., (6)), has a random coil structure (8), as has the *C* region in the full II-III loop in NMR analysis (Dulhunty and Casarotto, unpublished) or from structure predictions (24, 25). Thus the secondary structure of small regions of the II-III loop are retained in peptide fragments of the protein. An extrapolation of this finding is that functional effects of peptide fragments of the II-III loop on the RyR are likely to reflect functional changes which occur in more complex interactions between the intact DHPR and RyR in the whole cell.

5.4. Functional changes induced by changing peptide length

The results show that extension of a peptide fragment can lead to functional disruption, if the extended region exerts a stearic influence over the active region of the peptide. Indeed there are several examples in the literature in which small changes in the length of peptides corresponding to the *AB* region of the II-III loop have resulted in significant differences in peptide activity. A 61 amino acid peptide, SCDLf1 (residues 666-726) binds to RyR1 and activates the channel (26). The sequence from residues 671-690 (peptide *A*) activates Ca^{2+} release from skeletal SR and RyR channels (see Introduction). In contrast (a) a peptide corresponding to residues 666-709 of the skeletal DHPR (the s31 region) does not bind to RyR1 (27) and (b) peptide *AB* (residues 671-710) does not activate the channel (this study). In summary, the *A* region alone activates RyR1. Addition of the next 20 amino acids of native sequence abolishes activity. Addition of a further 16 residues of native sequence downstream and 5 residues upstream, restores activity (26). It is likely that, as in the *AB* peptide, the essential RKRRK residues in the *A* region of residues 666-709 (27) were compromised by the presence of the acidic *B* residues (in **D**KT**EEE**K). The DHPR fragment containing the A region may well have bound to the RyR if it had been either extended to residue 726 or truncated by to residue 691.

The recombinant II-III loop binds to the RyR and activates the channel (3, 28). This activation could occur through binding of either the *A* or the *C* region of the loop to the RyR, since both regions activate the channel under appropriate conditions (28). However, the fact that SCDLf1 (residues 666-726) is capable of activating the RyR shows that the A region can be active if the AB region is extended. This raises the possibility that the region can bind to the RyR in both the recombinant loop and in the intact protein (if it could be targeted to the RyR).

5.5. The role of the AB region in skeletal muscle EC coupling

There is unequivocal evidence that skeletal type EC coupling in myocytes, which occurs in the absence of extracellular Ca^{2+} influx, depends on the presence of a skeletal sequence in the DHPR II-III loop residues 725-740 (i.e. the N-terminal part of the C region as defined in (6)) (25, 29, 30). It is however not clear whether this *C* sequence is a requirement for the physical interaction

Table 3. Proton assignment and predicted secondary structure information based on α-^{1}H CSI information (α = alpha helical; β = beta sheet) for the AB_{LK} peptide in 18 % TFE, pH 5 at 25°C

Residue	NH	Hα	Hβ	Other	αH_i-CSI
Thr^{671}	8.21	4.46	4.36	Hγ 1.29	
Ser^{672}	8.66	4.29	4.01/3.97		
Ala^{673}	8.30	4.22	1.45		
Gln^{674}	7.96	4.03	2.21/2.29	Hγ 2.46/2.65, δNH_2 7.48/6.77	α
Lys^{675}	8.21	4.15	2.00/1.95	Hγ 1.47, Hδ 1.68, Hε 2.98, eNH_2 7.60	
Ala^{676}	8.09	4.14	1.50		
Lys^{677}	7.92	4.06	1.96	Hγ 1.46, Hδ 1.65, Hε 2.96, eNH_2 7.61	α
Ala^{678}	8.02	4.10	1.55		α
Glu^{679}	8.32	4.08	2.25/2.17	Hγ 2.56/2.46	α
Glu^{680}	8.18	4.10	2.23/2.16	Hγ 2.56/2.46	α
Arg^{681}	8.13	3.98	1.96/1.88	Hγ 1.62/1.70, Hδ 3.22, NH 7.25	α
Lys^{682}	7.92	4.00	1.96	Hγ 1.42, Hδ 1.57/1.70, Hε 2.96, eNH_2 7.60	α
Arg^{683}	8.26	4.04	1.95.1.90	Hγ 1.68, Hδ 3.20, NH 7.30	α
Arg^{684}	8.28	4.08	1.95	Hγ 1.69, Hδ 3.19, NH 7.34	α
Lys^{685}	8.44	4.26	1.85/1.81	Hγ 1.51/1.47, Hδ 1.63, Hε 3.01, eNH_2 7.62	
Met^{686}	8.12	4.22	2.12/2.18	Hγ 2.69/2.61, εCH_3 2.20	α
Ser^{687}	8.27	4.23	4.05/4.10		α
Arg^{688}	7.94	4.17	1.96/1.93	Hγ 1.70/1.74, Hδ 3.23, NH 7.26	α
Ala^{689}	8.04	4.20	1.54		
Leu^{690}	8.23	4.18	1.70	Hγ 1.67, Hδ 0.92/0.91	α
Ala^{691}	8.12	4.16	1.54		
Asp^{692}	8.39	4.51	3.00/2.86		α
Lys^{693}	8.18	4.11	1.92	Hγ 1.58, Hδ 1.68, Hε 2.96, eNH_2 7.58	α
Thr^{694}	8.25	4.34	4.00	Hγ 1.29	
Glu^{695}	8.18	4.10	2.23/2.17	Hγ 2.56/2.46	α
Glu^{696}	7.81	4.32	2.14/2.15	Hγ 2.41/2.56	
Glu^{697}	8.02	4.25	2.14/2.19	Hγ 2.51/2.63	
Lys^{698}	8.09	4.16	1.94	Hγ 1.47, Hδ 1.70, Hε 2.98, eNH_2 7.60	
Ser^{699}	7.92	4.17	4.06/4.00		α
Val^{700}	7.94	3.71	2.21	Hγ 0.97/1.08	α
Met^{701}	7.98	4.28	2.12/2.18	Hγ 2.60/2.69	
Ala^{702}	8.13	4.09	1.50		α
Lys^{703}	7.66	4.10	1.94	Hγ 1.49, Hδ 1.70, Hε 2.98, eNH_2 7.58	α
Lys^{704}	7.98	4.12	1.93	Hγ 1.50, Hδ 1.69, Hε 2.96, eNH_2 7.61	α
Leu^{705}	8.04	4.23	1.60	Hγ 1.58, Hδ 0.90/0.89	α
Glu^{706}	7.81	4.28	2.16	Hγ 2.58/2.71	
Gln^{707}	7.83	4.32	2.04/2.14	Hγ 2.41/2.46, Hδ 6.79/7.41	
Lys^{708}	8.03	4.59	1.86/1.79	Hγ 1.52, Hδ 1.72, Hε 3.03, eNH_2 7.58	β
Pro^{709}		4.44	2.33/2.04	Hγ 1.92, Hδ 3.65/3.86	
Lys^{710}	8.28	4.26	1.85/1.79	Hγ 1.51/1.47, Hδ 1.79/1.85, Hε 3.03, eNH_2 7.61	

between the RyR and DHPR, or for targeting the DHPR in an appropriate position to allow a physical interaction with the RyR. Disruption in either case would prevent any protein/protein interaction. The role of the *A* region in EC

Table 4. Proton NMR assignment and predicted secondary structure information based on α-^{1}H CSI information (α= alpha helical, ▼β= beta sheet) for the AB_{CH} peptide in 18 % TFE, pH 5.0 at 25°C

Residue	NH	Hα	Hβ	Other	αH_i-CSI
Thr^{671}	8.22	4.47	4.37	Hγ 1.32	α
Ser^{672}	8.66	4.32	4.03/3.98		
Ala^{673}	8.31	4.25	1.46		
Gln^{674}	7.99	4.07	2.23/2.11	Hγ 2.48/2.45, δNH_3 7.44/6.80	α
Lys^{675}	8.22	4.07	1.90	Hγ 1.56, Hδ 1.71, Hε 2.96, ζNH_3 7.60	α
Ala^{676}	8.10	4.17	1.51		
Lys^{677}	7.95	4.13	1.94	Hγ 1.47, Hδ 1.63/1.73, Hε 2.98, ζNH_3 7.61	α
Ala^{678}	8.04	4.13	1.56		
Glu^{679}	8.28	4.12	2.16/2.22	Hγ 2.61/2.53	α
Glu^{680}	8.12	4.10	2.11/2.22	Hγ 2.51/2.59	α
Arg^{681}	8.15	4.04	1.95/1.87	Hγ 1.65/1.78, Hδ 3.23, NH 7.23	α
Lys^{682}	7.93	4.11	1.94	Hγ 1.44, Hδ 1.58/1.73, Hε 2.97, ζNH_3 7.60	α
Arg^{683}	8.20	4.11	1.94/1.90	Hγ 1.66/1.78, Hδ 3.22, NH 7.29	α
Arg^{684}	8.15	4.15	1.94	Hγ 1.69, Hδ 3.21, NH 7.42	α
Lys^{685}	8.05	4.18	1.91/1.87	Hγ 1.55, Hδ 1.71, Hε 3.01, ζNH_3 7.62	
Met^{686}	8.18	4.43	2.19	Hγ 2.62/2.72, εCH_3 2.20	
Ser^{687}	8.02	4.43	3.98/3.96		
Arg^{688}	8.02	4.38	1.97/1.85	Hγ 1.71/1.75, Hδ 3.24, NH 7.23	
Gly^{689}	8.22	4.00			
Leu^{690}	8.00	4.62	1.69/1.59	Hγ 1.60, Hδ 0.98/0.96	β
Pro^{691}		4.43	2.35/2.20	Hγ 2.06, Hδ 3.67/3.85	
Ala^{692}	8.14	4.29	1.46		
Lys^{693}	8.31	4.23	1.90	Hγ 1.55, Hδ 1.71, Hε 3.00, ζNH_3 7.62	
Thr^{694}	7.94	4.24	4.13	Hγ 1.29	α
Ala^{695}	7.95	4.22	1.50		
Val^{696}	7.90	3.83	2.15	Hγ 2.20, Hδ 1.05/0.96	α
Ala^{697}	8.14	4.12	1.49		
Lys^{698}	8.19	4.09	1.94	Hγ 1.46, Hδ 1.67, Hε 2.95, ζNH_3 7.60	α
Ser^{699}	7.93	4.32	3.94		
Val^{700}	8.11	3.81	2.20	Hγ 0.99/1.09	α
Met^{701}	8.16	4.24	2.19/2.13	Hγ 2.62/2.70	
Ala^{702}	8.08	4.12	1.50		
Lys^{703}	7.74	4.14	1.94	Hγ 1.49, Hδ 1.62, Hε 3.01, ζNH_2 7.58	α
Lys^{704}	8.06	4.19	1.90	Hγ 1.47/1.50, Hδ 1.71, Hε 2.98, ζNH_3 7.61	
Leu^{705}	8.06	4.27	1.61/1.80	Hγ 1.57, Hδ 0.90/0.93	
Glu^{706}	7.87	4.28	2.18/2.13	Hγ 2.54/2.63	
Gln^{707}	7.89	4.34	2.44/2.42	Hγ 2.42/2.54, Hδ 6.80/7.50	
Lys^{708}	8.08	4.62	1.87/1.80	Hγ 1.53, Hδ 1.72/1.74, Hε 3.05, ζNH_3 7.58	β
Pro^{709}		4.46	2.34	Hγ 1.94, Hδ 3.67/3.87	
Lys^{710}	8.02	4.27	1.86/1.80	Hγ 1.52, Hδ 1.73, Hε 3.04, eNH_2 7.61	

coupling has not been established. Clearly, skeletal EC coupling can occur in the absence of the region, or when it is severely scrambled (29-31). However removal of both the *A* and *C* residues allows some recovery of skeletal EC coupling

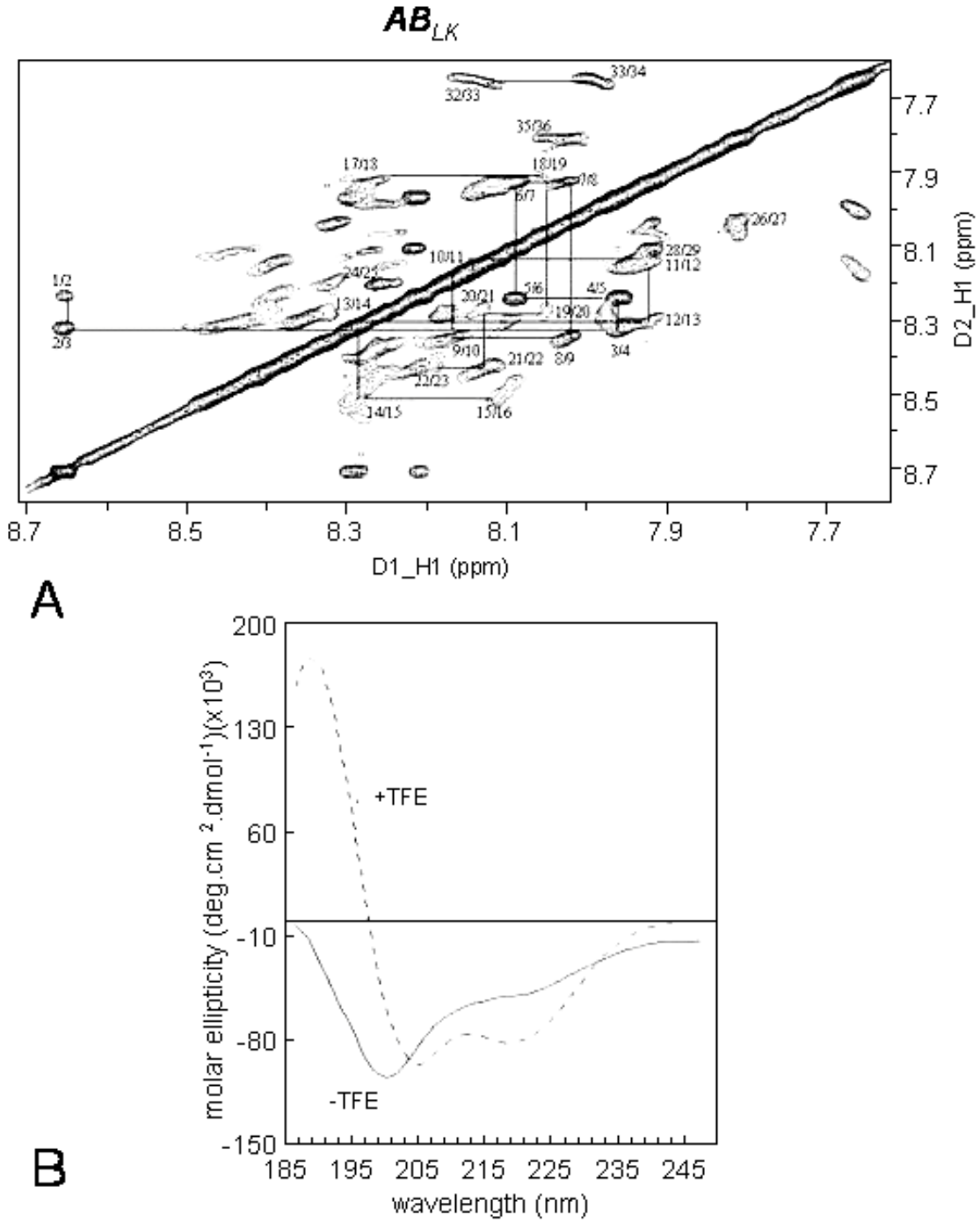

Figure 5. The structure of AB_{LK} determined using NMR and CD analysis is similar to that of the native AB peptide, with more structure in the linker region. The amide-amide region of the AB_{LK} peptide NOESY spectrum in 82% H_2O/18 % d_{18} TFE) is shown in (**A**) indicates the peptide adopts an α-helical secondary structure. Strong and continuous i-i+1 NOEs are shown and correspondingly labeled (1-36). The region 18-22 now forms part of the helical structure. (**B**) - CD spectra at 5°C for AB_{LK} in 100% H_2O (solid line) and 82% H_2O/18 % TFE (dashed line)

(31), suggesting that the *A* region contributes to the DHPR/RyR interaction and contributes to the overall protein/protein interaction.

The results of this study suggest that the conformation of the II-III loop could provide a switch that allows the *A* region to interact with the RyR. If the conformation is such that the positive charge of the A region is neutralized by negative charges in the B region then an interaction is precluded. A change in conformation

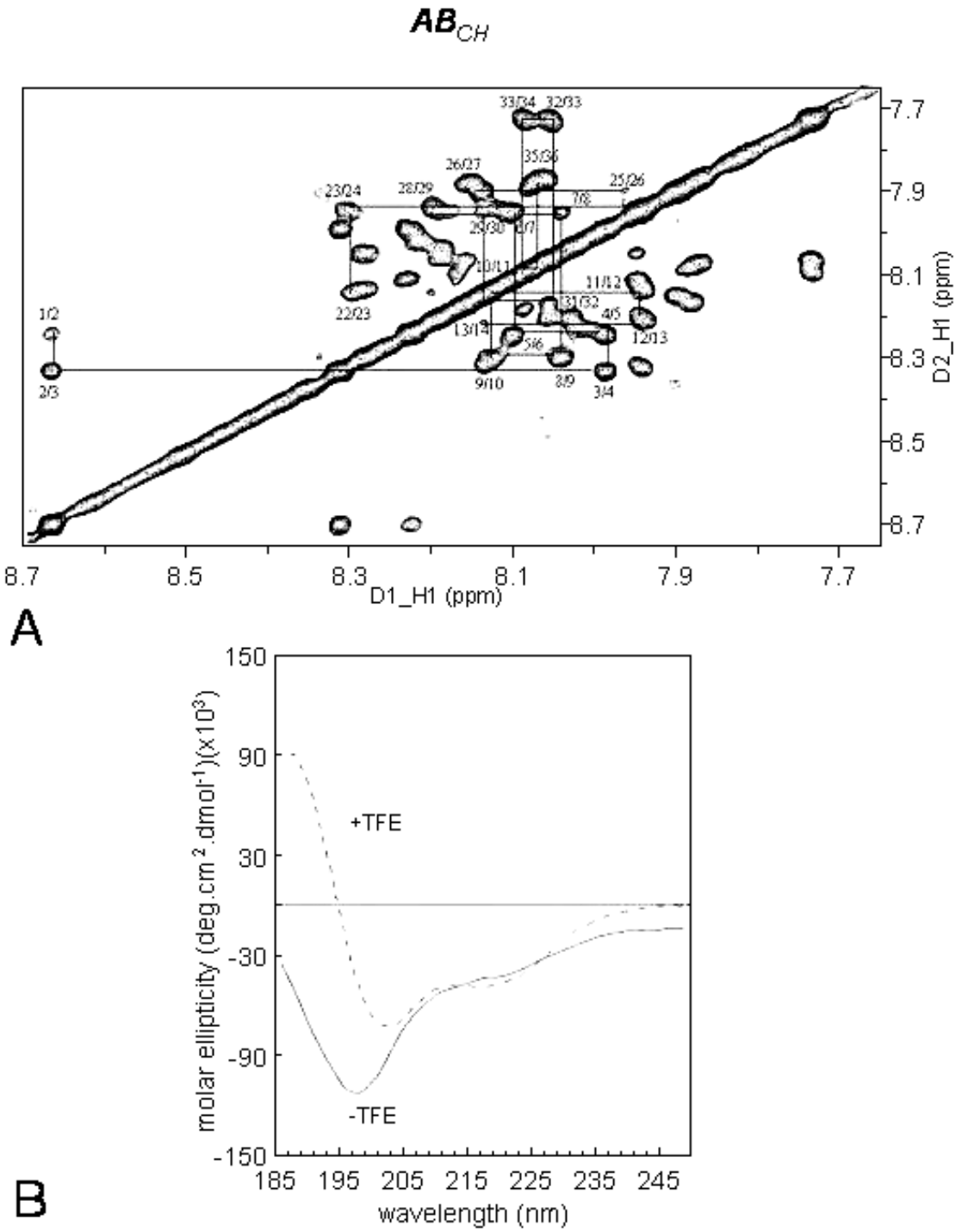

Figure 6. The amide-amide region of the AB_{CH} NOESY spectrum in 82% H_2O/18 % d_{18} TFE shown in (**A**) indicates that the peptide adopts an α-helical secondary structure with strong and contiguous i-i+1 NOE crosspeaks between residues 1-14 and 22-36 (**B**) - CD spectra at 5°C of the AB_{CH} in 100% H2O (solid line) and 82% H_2O/18 % TFE (dashed line).

that removed this neutralizing effect would allow *A* region to interact. Such a change in conformation could contribute to functional changes associated with EC coupling or with retrograde signaling.

In conclusion, we predicted that the 40 amino acid *AB* peptide corresponding to residues 671-710 of the II-III loop in the α_1 subunit of the skeletal DHPR would be a strong activator of the skeletal RyR1 channel, because (a) it contained a sequence of basic residues that had previously been shown to be responsible for high affinity activation of the RyR and (b) we predicted that the

structure of the activating region would further resemble the full II-III loop. Although the structure of the activating region was maintained, the 40 residue peptide had no functional activity. Strong activity was restored when negatively charged residues in the C-terminal part of the peptide were replaced by neutral residues. The results suggest that the affinity of the *A* region of the skeletal II-III loop for the RyR might depend on the overall conformation of the II-III loop, which is thought to change during EC coupling.

6. REFERENCES

1. Green, D., S. Pace, S. M. Curtis, M. Sakowska, G. D. Lamb, A.F. Dulhunty and M.G. Casarotto: The three-dimensional structural surface of two beta-sheet scorpion toxins mimics that of an alpha-helical dihydropyridine receptor segment. *Biochem J* 370, 517-27 (2003)

2. Tanabe, T., K.G. Beam, B.A. Adams, T. Niidome and S. Numa: Regions of the skeletal muscle dihydropyridine receptor critical for excitation-contraction coupling. *Nature* 346, 567-9 (1990)

3. Lu, X., L. Xu and G. Meissner: Activation of the skeletal muscle calcium release channel by a cytoplasmic loop of the dihydropyridine receptor. *The Journal of Biological Chemistry* 269, 6511-6516 (1994)

4. Dulhunty, A.F., D.R. Laver, E.M. Gallant, M.G. Casarotto, S.M. Pace and S. Curtis: Activation and inhibition of skeletal RyR channels by a part of the skeletal DHPR II-III loop: effects of DHPR Ser687 and FKBP12. *Biophys J* 77, 189-203 (1999)

5. Dulhunty, A.F., S.M. Curtis, S. Watson, L. Cengia and M.G. Casarotto: Multiple Actions of Imperatoxin A on Ryanodine Receptors: INTERACTIONS WITH THE II-III LOOP "A" FRAGMENT. *J Biol Chem* 279, 11853-62 (2004)

6. El-Hayek, R., B. Antoniu, J. Wang, S.L. Hamilton and N. Ikemoto: Identification of calcium release-triggering and blocking regions of the II-III loop of the skeletal muscle dihydropyridine receptor. *The Journal of Biological Chemistry* 270, 22116-22118 (1995)

7. Gurrola, G.B., C. Arevalo, R. Sreekumar, A.J. Lokuta, J.W. Walker and H.H. Valdivia: Activation of ryanodine receptors by imperatoxin A and a peptide segment of the II-III loop of the dihydropyridine receptor. *J Biol Chem* 274, 7879-86 (1999)

8. Haarmann, C.S., D. Green, M.G. Casarotto, D.R. Laver and A.F. Dulhunty: The random-coil 'C' fragment of the dihydropyridine receptor II-III loop can activate or inhibit native skeletal ryanodine receptors. *Biochem J* 372, 305-16 (2003)

9. Stange, M., A. Tripathy and G. Meissner: Two domains in dihydropyridine receptor activate the skeletal muscle Ca(2+) release channel. *Biophys J* 81, 1419-29 (2001)

10. Yamamoto, T., J. Rodriguez and N. Ikemoto; Ca2+-dependent dual functions of peptide C. The peptide corresponding to the Glu724-Pro760 region (the so-called determinant of excitation-contraction coupling) of the dihydropyridine receptor alpha 1 subunit II-III loop. *J Biol Chem* 277, 993-1001 (2002)

11. Casarotto, M.G., F. Gibson, S.M. Pace, S.M. Curtis, M. Mulcair and A.F. Dulhunty, A structural requirement for activation of skeletal ryanodine receptors by peptides of the dihydropyridine receptor II-III loop. *J Biol Chem* 275, 11631-7 (2000)

12. Casarotto, M.G., D. Green, S.M. Pace, S.M. Curtis and A.F. Dulhunty: Structural determinants for activation or inhibition of ryanodine receptors by basic residues in the dihydropyridine receptor II-III loop. *Biophys J* 80, 2715-26 (2001)

13. Kumar, A., R.R. Ernst and K. Wuthrich: A two-dimensional nuclear overhauser enhancement (2D nOe) experiment for the elucidation of complete proton-proton cross-relaxation networks in biological molecules. *Biochem Biophys Res Commun* 95, 1-6 (1980)

14. Bax, A. and D.G. Davis: MLEV-17 based two dimensional homonuclear magnetisation transfer spectroscopy. *J Magn Reson* 65, 355-360 (1985)

15. Rance, M., O.W. Sorensen, G. Bodenhausen, G. Wagner, R.R. Ernst and K. Wuthrich, Improved spectral resolution in COSY 1H NMR spectra of proteins via double quantum filtering. *Biochem Biophys Res Commun* 117, 479-83 (1983)

16. Deslauriers, R. and I.C.P. Smith: Biological Magnetic Resonance, 2nd Ed ed., Plenum Press, New York (1980)

17. Brunger, A.T., G.M. Clore, A.M. Gronenborn and M. Karplus: *Proceedings of the National Academy of Science USA* 83, 3801-3805 (1986)

18. Brunger, A.T: X-PLOR: A system for X-ray Crystallography and NMR. Version 3.1, Yale University, New Haven, CT (1992)

19. Buck, M., S.E. Radford and C.M. Dobson: A partially folded state of hen egg white lysozyme in trifluoroethanol: structural characterization and implications for protein folding. *Biochemistry* 32, 669-78 (1993)

20. Slupsky, C.M., C.M. Kay, F.C. Reinach, L.B. Smillie and B.D. Sykes: Calcium-induced dimerization of troponin C: mode of interaction and use of trifluoroethanol as a denaturant of quaternary structure. *Biochemistry* 34, 7365-75 (1995)

21. Wishart, D. S., B. D. Sykes and F. M. Richards: Realtionship between nuclear magnetic resonance chemical shift and protein secondary structure. *J Mol*

Biol 222, 311-33 (1991)

22. Fajloun, Z., R. Kharrat, L. Chen, C. Lecomte, E. Di Luccio, D. Bichet, M. El Ayeb, H. Rochat, P.D. Allen, I.N. Pessah, M. De Waard and J.M. Sabatier: Chemical synthesis and characterization of maurocalcine, a scorpion toxin that activates Ca (2+) release channel/ryanodine receptors. *FEBS Lett* 469, 179-85 (2000)

23. Dulhunty, A.F., S.M. Curtis, L. Cengia, M. Sakowska and M.G. Casarotto: Peptide fragments of the dihydropyridine receptor can modulate cardiac ryanodine receptor channel activity and SR Ca 2+ release. *Biochem J* 379. 161-72 (2004)

24. Bannister, M.L., A.J. Williams and R. Sitsapesan: Removal of clustered positive charge from dihydropyridine receptor II-III loop peptide augments activation of ryanodine receptors. *Biochem Biophys Res Commun* 314, 667-74 (2004)

25. Kugler, G., R.G. Weiss, B.E. Flucher and M. Grabner: Structural requirements of the dihydropyridine receptor alpha1S II-III loop for skeletal-type excitation-contraction coupling. *J Biol Chem* 279, 4721-8 (2004)

26. X. Lu, L. Xu and G. Meissner: Phosphorylation of dihydropyridine receptor II-III loop peptide regulates skeletal muscle calcium release channel function. Evidence for an essential role of the beta-OH group of Ser687. *J Biol Chem* 270, 18459-64 (1995)

27. Proenza, C., J. O'Brien, J. Nakai, S. Mukherjee, P.D. Allen and K.G. Beam: Identification of a region of RyR1 that participates in allosteric coupling with the alpha (1S) (Ca (V)1.1) II-III loop. *J Biol Chem* 277, 6530-5 (2002)

28. Dulhunty, A.F., C.S. Haarmann, D. Green, D.R. Laver, P.G. Board and M.G. Casarotto: Interactions between dihydropyridine receptors and ryanodine receptors in striated muscle. *Prog Biophys Mol Biol* 79, 45-75 (2002)

29. Proenza, C., C.M. Wilkens and K.G. Beam, Excitation-contraction coupling is not affected by scrambled sequence in residues 681-690 of the dihydropyridine receptor II-III loop. *J Biol Chem* 275, 29935-7 (2000)

30. Wilkens, C.M., N. Kasielke, B.E. Flucher, K.G. Beam and M. Grabner, Excitation-contraction coupling is unaffected by drastic alteration of the sequence surrounding residues L720-L764 of the alpha 1S II-III loop. *Proc Natl Acad Sci USA* 98, 5892-7 (2001)

31. Ahern, C.A., D. Bhattacharya, L. Mortenson and R. Coronado: A component of excitation-contraction coupling triggered in the absence of the T671-L690 and L720-Q765 regions of the II-III loop of the dihydropyridine receptor alpha (1s) pore subunit. *Biophys J* 81, 3294-307 (2001)

Key Words: dihydropyridine receptor, II-III loop, ryanodine recptor, NMR structure, peptide

Send correspondence to: Dr Marco G. Casarotto, Division of Molecular Bioscience, John Curtin School of Medical Research, Australian National University, P. O. Box 334, ACT 2601, Australia, Tel: 61-2-61252598, Fax: 61-2-61250415, E-mail: Marco.Casarotto@anu.edu.au